Final published version of this article: Applied Surface Science, Volume 590 (2022), 153067
Available online: 12 March 2022
https://doi.org/10.1016/j.apsusc.2022.153067

Fast-tracking of NH_3 interaction with ZnO nanorods and C/ZnO hybrid nanostructures by operando spectroscopy

Puleng N Mbuyisa[a*], Federica Rigoni[b,e], Silvia Nappini[c], Elena Magnano[c,f], Stefania Pagliara[b], Giovanni Drera[b] , Luigi Sangaletti[b], Andrea Goldoni[d], Muzi Ndwandwe[a], Cinzia Cepek[c]

[a] *Department of Physics and Engineering, University of Zululand, Private Bag X1001, Kwadlangezwa 3886, South Africa*

[b] *Interdisciplinary Laboratories for Advanced Materials Physics and Dipartimento di Matematica e Fisica, Università Cattolica del Sacro Cuore, via dei Musei 41 I-25121 Brescia, Italy*

[c] *Istituto Officina dei Materiali-CNR, Laboratorio TASC, s.s. 14, km 163.4 I-34149 Trieste, Italy*

[d] *Elettra—Sincrotrone Trieste S.C.p.A, s.s. 14, km 163.4 I-34149 Trieste, Italy*

[e] *Department of Molecular Sciences and Nanosystems, Ca' Foscari University of Venice, via Torino 155, 30170 Venezia-Mestre, Italy*

[f] *Department of Physics, University of Johannesburg, P.O. Box 524, Auckland Park, Johannesburg 2006, South Africa*

Abstract

Fast X-ray photoemission spectroscopy has been carried out to track the interaction of ammonia gas with hybrid materials based on ZnO nanorods and nanostructured carbon. We provide, for the first time, direct evidence of gas adsorption of ammonia on nanostructured hybrid interfaces combining photoemission with transport measurements through the resistivity change upon gas exposure. This operando methodology allowed us to reconstruct the adsorption isotherms and relate the different

[*] Department of Physics and Engineering, University of Zululand, Private Bag X1001, Kwadlangezwa 3886, South Africa
Email:p.nmbuyisa@gmail.com

behavior to the sample morphology at the nanoscale. While on bare ZnO nanorods, physisorption of ammonia is detected along with photon beam assisted cracking, on the nanostructured carbon the formation of amine groups is detected, without displaying any effect induced by photon beam exposure. Our results make the present experiment an operando general methodology, with the possibility to relate the transport versus dose curves (ultimately the adsorption isotherms) to a specific investigation of the gas/surface interactions.

Keywords: ZnO**,** C/ZnO hybrid, NH_3 gas, fast acquisition XPS, adsorption isotherms, resistance

1. Introduction

Gas sensing represents one of the most important fields where carbon/metal oxide hybrids nanostructures are efficiently applied [1]. Carbon nanostructures (CNs) and nanostructured metal oxides, such as nanorods (NRs), are both individually used to detect gases and they are excellent complementary materials to create heterojunctions [2-8]. When combined in hybrid structures, they compensate for the shortcomings of the single components and their combination creates new advantageous features. Despite intensive research to advance the understanding of these materials, the complex array of possible CNs shapes and different metal oxides present several virtually unexplored areas. Specific real-time spectroscopic study of adsorption processes aimed to identify the dominant interactions between gas molecules and nanostructured surfaces and hybrids are still rare. Operando methodologies would enable the investigation of the adsorption isotherms, relating them to the sample morphology at the nanoscale.

Among carbon/metal oxide hybrids, heterointerfaces of ZnO and CNs have received much attention [9-14] due to the possibility to tune the morphology of the samples through the binary ZnO-C system down to the nanoscale. Furthermore, the capability to adsorb molecules on the surface makes these hybrids also interesting for gas storage applications and, in our particular case, for ammonia storage [15].

In this paper, the adsorption and desorption chemistry of ammonia gas on the ZnO NRs and CNs/ZnO hybrid grown using ZnO NRs as a template (C/ZnO) were studied by fast-acquisition XPS. The high energy-resolution of the photoemission probe used, along with the high photon flux and the tunable photon energy, allowed us to understand some of the mechanisms governing the interaction of the C/ZnO hybrid nanomaterials with NH_3 gas. Our data showed that ammonia chemisorbs on the hybrid C/ZnO structure, while it physisorbs on the bare ZnO NRs.

While acquiring fast-XPS data, the samples electrical resistance was collected and the adsorption isotherms were determined by considering the resistance change of the hybrid layers upon ammonia adsorption. This makes the present experiment an operando methodology, with the possibility to relate the transport versus dose curves (ultimately the adsorption isotherms) to a specific investigation of the NH_3/surface interaction. The adsorption isotherms showed for the bare ZnO NRs a steady increase and reached saturation at 400 L (1 L = 10^{-6} Torr), while for the C/ZnO hybrid the isotherms displayed two steps in the 0-400 L range. The curve of the C/ZnO hybrid displayed features quite similar to those observed for NH_3 chemisorption on mesoporous carbon [16], while, the curve of the bare ZnO nanorods displayed a behavior similar to that of physisorption by microporous solids [17].

2. Experimental

2.1 Synthesis of ZnO and C/ZnO hybrid nanostructures

The ZnO NRs were hydrothermally synthesized using a method developed by Wang et al [18]. This method involves the deposition of a thin film of ZnO on a silicon substrate prior to the hydrothermal growth. The film acts as the nucleation site for the NRs growth and ensures the vertical alignment of the grown NRs, as described in details in [19]. To synthesize the C/ZnO hybrid, the CVD process was carried out on the ZnO NRs at 800 ^{o}C using 50 sccm C_2H_2, see [20] for more details.

2.2 Characterization

The ZnO NRs and C/ZnO hybrid were characterized by SEM and XPS, ex-situ. The morphology of the nanostructures was studied using a 30 μm aperture SEM at 10 kV. The interaction of NH_3 gas with the nanostructures, was investigated by fast acquisition mode XPS during gas exposure and desorption using synchrotron radiation at the beamline for advanced circular dichroism (BACH) at Elettra. The XPS spectra were acquired at a rate of 300 ms per spectrum using a calibrated Scienta R3000 electron analyzer [21]. The photon energy could be tuned between 45-1600 eV with high resolving power of 2000-6000 in the entire energy range. Each sample was first heated in the preparation chamber to remove surface contaminants (~350-400°C), and then moved to the measurement chamber, where it was exposed to NH_3 at RT at different pressures (in the 10^{-7} - 10^{-5} mbar range). We performed the experiment using a leak valve, hence the range in pressure, we tried to expose the sample to the lowest possible pressure because for environmental monitoring it is important to detect the lowest possible concentration of a gas. During gas exposure the electrical resistance of the sample was measured, along with the C 1s, Zn 3d, O 1s, and N 1s XPS core level spectra.

Photon damage was checked and excluded by systematically moving the beam spot in sample areas not yet illuminated by the beam. After the measurements the sample was heated to remove the adsorbed ammonia, checking the decrease of the N1s intensity until its complete disappearance.

3. Results and discussion

3.1 Morphology

The deposition of a thin ZnO film on the silicon substrate prior to the hydrothermal process resulted in the growth of vertically aligned ZnO NRs with a pointed hexagonal shape at the end of the c-axis as previously described [18, 20], and shown in Figure 1a. The shape of the NRs is due to the etching effect during growth [18, 22]. The as grown nanorods are ~ 1µm in length and their diameter vary in the range of 50 to 200 nm. The C_2H_2 CVD process on the ZnO NRs resulted in the etching of the ZnO NRs and in the synthesis of 1-D carbon nano-dendrites, preferentially aligned along the location

of the ZnO nanorods [18], see Figure 1b. During the CVD process C_2H_2 decomposes to carbon and hydrogen and reacts with the ZnO nanorods forming adsorbed carbon and decomposition products which includes Zn, H_2O, CO and CO_2, which are in the gas phase during CVD

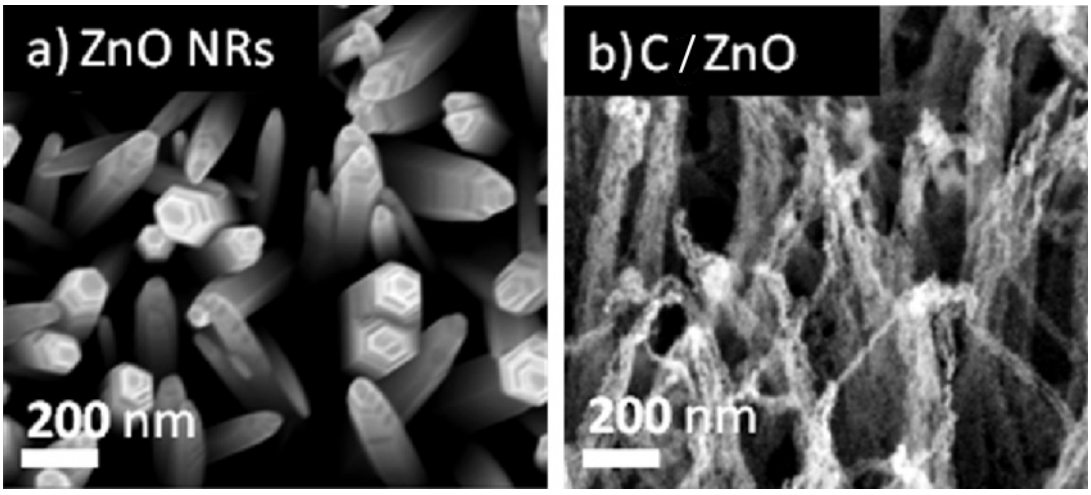

Figure 1: SEM micrographs of a) ZnO NRs grown by the hydrothermal method, b) C/ZnO hybrid nanostructures grown at 800 °C using the ZnO NRs as template.

3.2 Fast XPS during ammonia gas exposure

3.2.1 Bare ZnO NRs

The ZnO NRs were first annealed at ~350-400 °C in UHV (Ultra High Vacuum) before ammonia exposure to remove contaminants from the hydrothermal process and air exposure. The O 1s spectrum of the ZnO NRs after annealing (Figure 2a) is mainly composed of two peaks at binding energy (BE) 530.85 and 531.95 eV which can be assigned to O of Zn-O and hydroxyl groups, respectively [23-25].

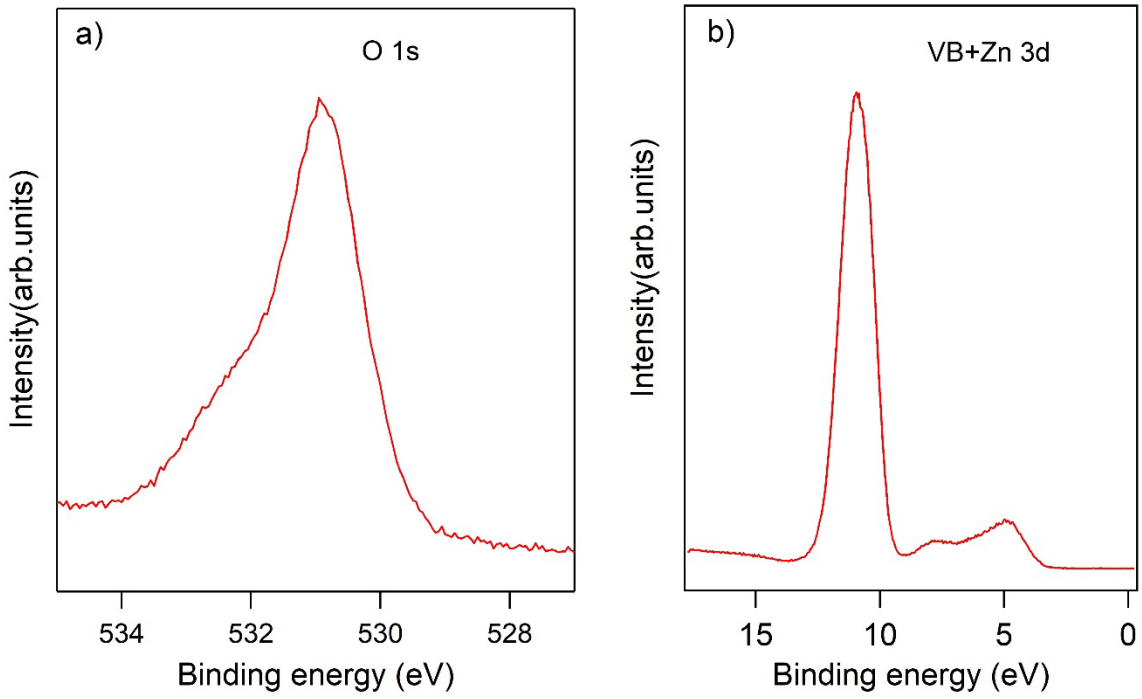

Figure 2: XPS spectra of a) O 1s and b) valence band, including the Zn 3d level at ~11eV, of the ZnO NRs after degassing at ~350°C. The spectra have been acquired using a photon energy of 605 eV, with an overall resolution of ~0.2 eV.

In Figure 3 (top left), a two-dimensional plot of the N 1s XPS spectra acquired using a photon energy of 605 eV during NH_3 gas exposure at ~10^{-5} mbar is shown, where the x-axis corresponds to the photoelectron BE, the y-axis to the exposure time (in seconds) and the figure color scale corresponds to the XPS intensity (black minimum, yellow maximum). On the right, single spectra extracted from the 2D plot (each acquired in ~300 ms) at selected significant time, before and during dosing, are shown. It is evident from Figure 3 that as soon as NH_3 starts to be dosed (time = 0 s) a peak at ~ 400.67 eV appears. The NH_3 dosing was stopped after ~2 s, in correspondence to the peak intensity dropping again to 0, as shown on the bottom left spectrum. According to literature [7], the peak observed at BE = 400.67 eV can be ascribed to physisorbed ammonia [26].

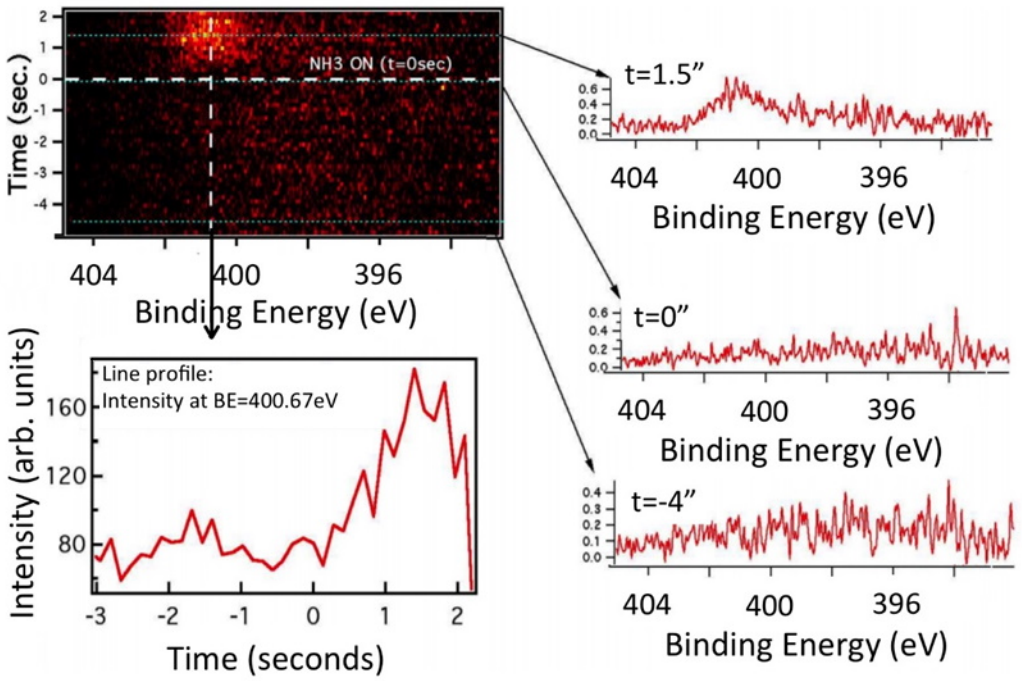

Figure 3: Two-dimensional fast XPS spectra of the N 1s level acquired at RT during NH_3 dosing at ~10^{-5} mbar (black: minimum intensity, yellow maximum intensity) on the ZnO NRs. Each spectrum has been acquired using an acquisition time of ~300 ms, with the analyzer in fixed energy mode at a pass energy of 50 eV. Time = 0 s corresponds to the time when gas exposure started.

When XPS measurements were performed during NH_3 dosing at lower pressure ($5x10^{-7}$ mbar) and for longer time (~414 seconds), a progressive growth of an additional peak at lower BEs (~398.9 eV) was observed, as shown in Figure 4. The lower energy component’s intensity increased until it becomes the dominant peak after 410 seconds of exposure.

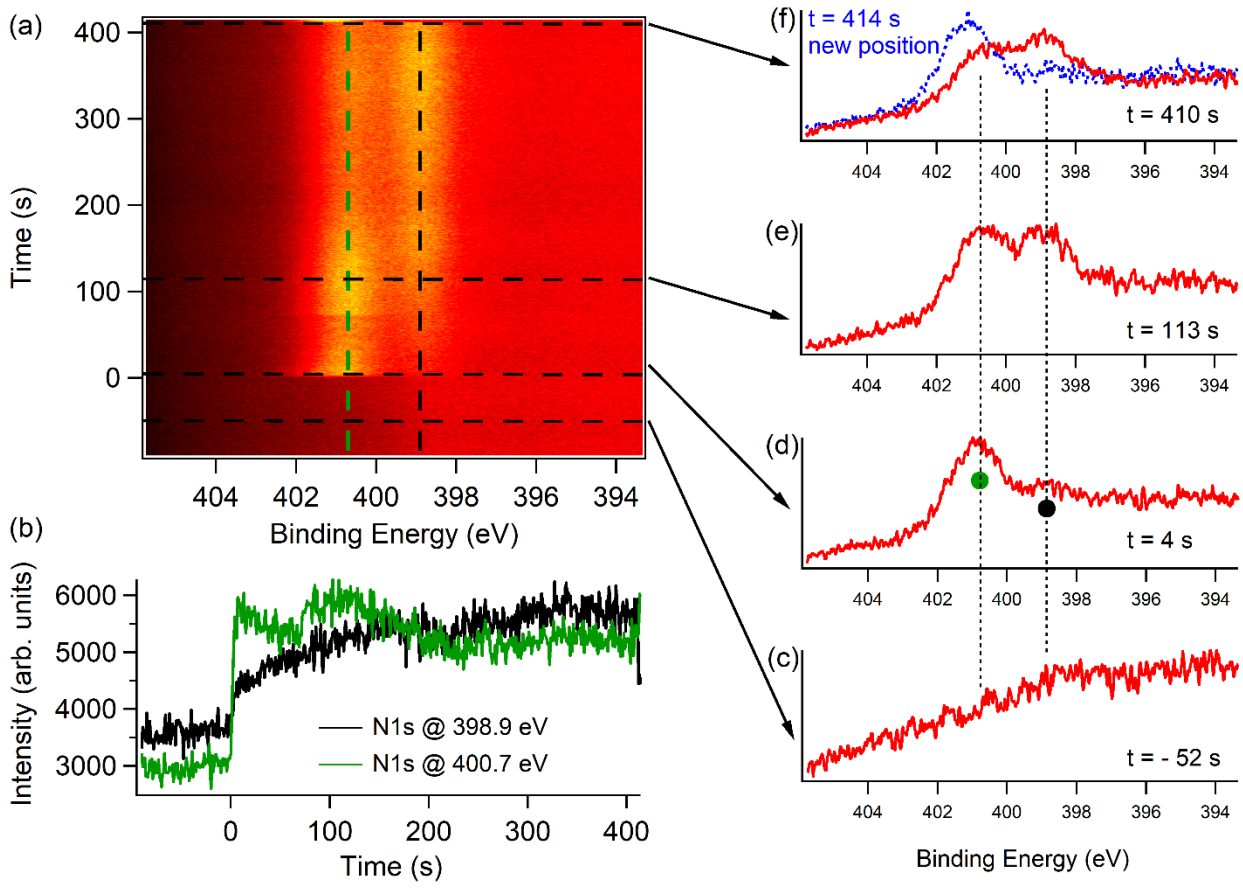

Figure 4: (a) Two-dimensional fast XPS spectra of the N 1s level acquired at RT during NH_3 dosing at ~$5x10^{-7}$ mbar (black: minimum intensity, yellow maximum intensity) on the ZnO NRs. Each spectrum has been acquired in ~300 ms using the analyzer fixed-energy mode and a pass energy of 50 eV. (b) Vertical line profile showing XPS signal versus time related to peak energy of 400.7 eV (green line) and 398.9 eV (black line). (c-f) Horizontal line profile showing XPS spectra at different time (peaks at 400.7 eV and 398.9 eV are highlighted by dashed vertical lines and green and black dots in panel d).

When the measuring position on the sample was changed, by displacing the sample holder by a few mm (see Figure 4, top right, blue spectrum), the higher energy component became again the dominant peak. This suggests that the photon beam has induced the cracking of the NH_3 molecules and the physisorption of these products on the ZnO NRs surface. The increase of the lower BE peak intensity with beam exposure duration is similar to that reported for electron bombardment [27] and heat [28]

stimulated dissociation of ammonia. We note that the N 1s peak observed after changing the sample holder position (blue line Figure 4f) is shifted by ~0.5 eV to higher binding energy with respect to the initial one (t=4 s, Figure 4d). A possible explanation can be that the sample was not homogeneous on a scale compatible with the dimension of the photon beam (~ 250 x 250 μm^2). In addition the first peak has been observed dosing during photon exposure, which can damage the adsorbed ammonia on a time-scale lower than the spectra acquisition time (300 ms.).

In order to clarify this aspect and compare the thermal effect with that induced only by the photon beam, fast XPS spectra of N1s core level were recorded on NH_3-exposed ZnO during annealing at 100 °C (see Figure 5). The analysis of the 2D fast XPS spectra of thermal treated sample in Figure 5 shows that the peak at 400.7 eV is less intense than that of unheated sample in Figure 4. This peak completely disappeared after 100 s of heating at 100°C, while the intensity of the peak at 398.8 eV is reduced but not completely quenched even after 200 s of heating. A new minor component at 397.8 eV, due to thermal decomposition of NH_3, was also observed.

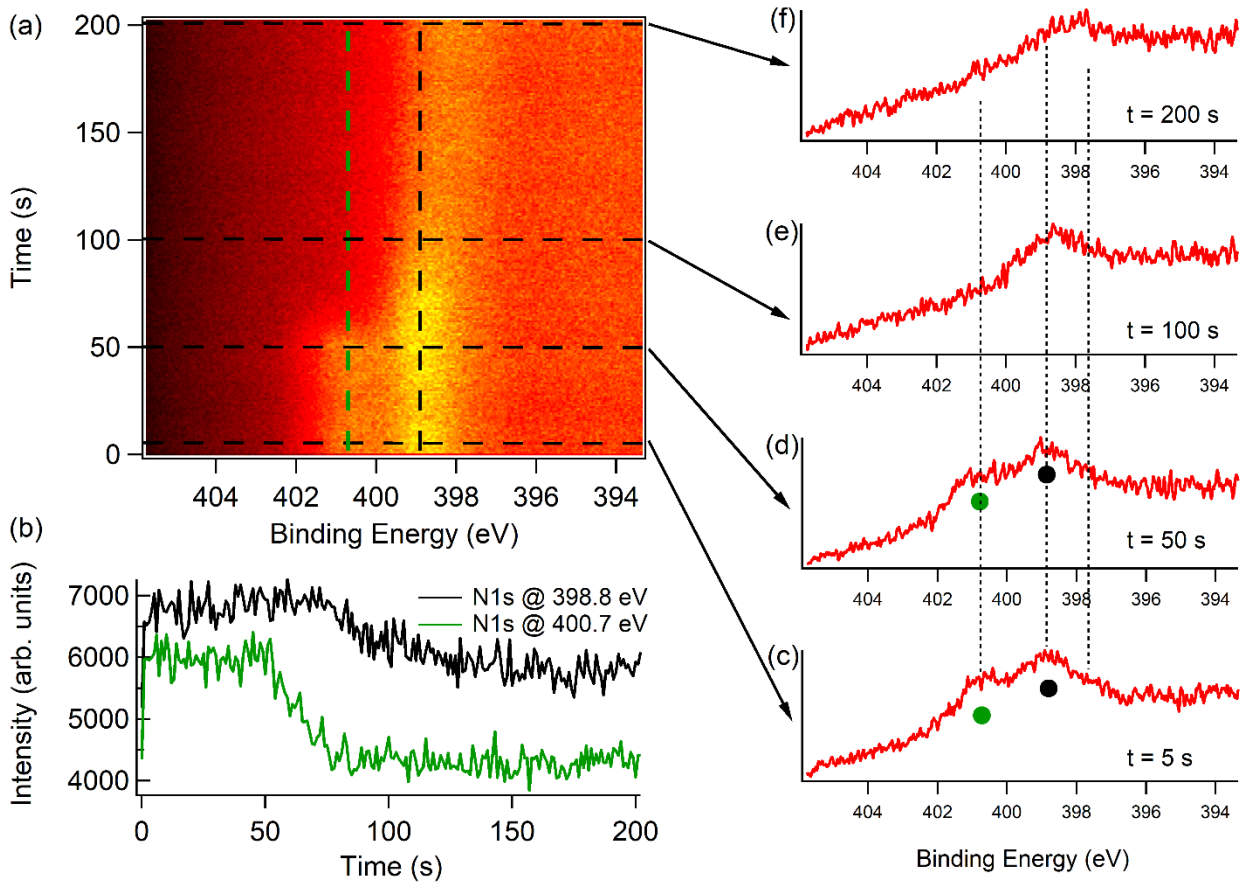

Figure 5: (a) Fast XPS spectra of the N 1s level with the corresponding intensity variations (black: minimum intensity, yellow maximum intensity) with time acquired during annealing the ZnO NRs sample at ~100 °C (left panel). (b) Vertical line profile showing XPS signal versus time related to peak energy of 400.7 eV (green line) and 398.8 eV (black line). (c-f) Selected single spectra extracted from the 2D plot are also shown on the right panel. In addition to the peaks at 400.7 eV and 398.8 eV, also observed in the Figure 4, a minor component at around 397.8 eV, due to decomposition products, is highlighted by a third dashed vertical line.

Based on the results discussed above, we therefore assign the peak at 400.7 eV to physisorbed ammonia and the low BE N 1s peaks (the main at 398.8 eV and a minor component at around 397.8 eV) to ammonia decomposition products [26, 29, 30].

In addition, as further confirmation of physisorption mechanism of NH_3 molecule on ZnO surface, the O 1s and Zn 3d peaks of ZnO were measured (Figure 6) during NH3 exposure before the N 1s

saturation was reached. For both elements no change in the line shape or peak position was observed or the formation of zinc nitride even after 330 seconds of exposure.

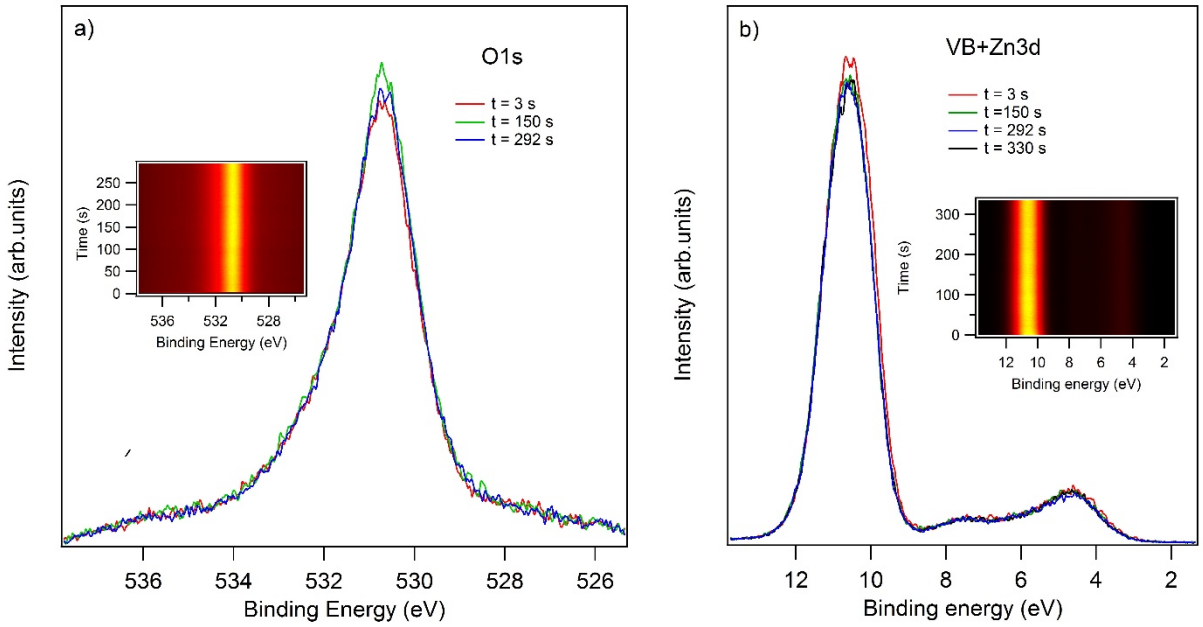

Figure 6: Fast XPS (a) O1s and (b) valance band plus Zn 3d level during ammonia exposure, before the saturation of the N 1s signal was detected. Their corresponding 2D plots are reported as inserts.

From these results we can conclude that ammonia is physisorbed on the ZnO NRs. The NH_3 physisorption process is very fast, detectable in a time-scale of ~100 milliseconds, and the sample reacts in UHV at very low doses of NH_3, showing visible modifications in the N 1s core level upon an exposure of 7.5×10^{-2} Langmuir (1 second at 10^{-7} mbar).

3.2.2 C/ZnO hybrid nanostructures

When the C/ZnO hybrid was exposed to ammonia gas for ~ 2400 seconds at ~10^{-7} mbar, the chemisorption of ammonia with formation of amine groups was observed after about 800 sec. This is indicated by the appearance of the N 1s peak at 398.9 eV, see Figure 7, which corresponds to

chemically bound nitrogen in the form of NH_x species [31], while no sign of NH_3 physisorption was detected. The chemical interaction between amine group species and C/ZnO hybrid is also visible in C1s core level (see Figure 8), where the broadening of the spectrum can be ascribed to the emergence of a new component at ~286 eV, most likely related to the formation of C-N bond [32]. The N 1s peak remained at the same BE even if the sample position was changed or if NH_3 was dosed without exposing the sample to the photon beam, using the same procedure as for the bare NRs. This indicates that the ammonia is not affected or dissociated by the photon beam, unlike the case of the bare ZnO NRs previously discussed. It should be noted that for this sample a lower resolution was used as compared to the NRs, hence the spectra appear broader than the previous ones.

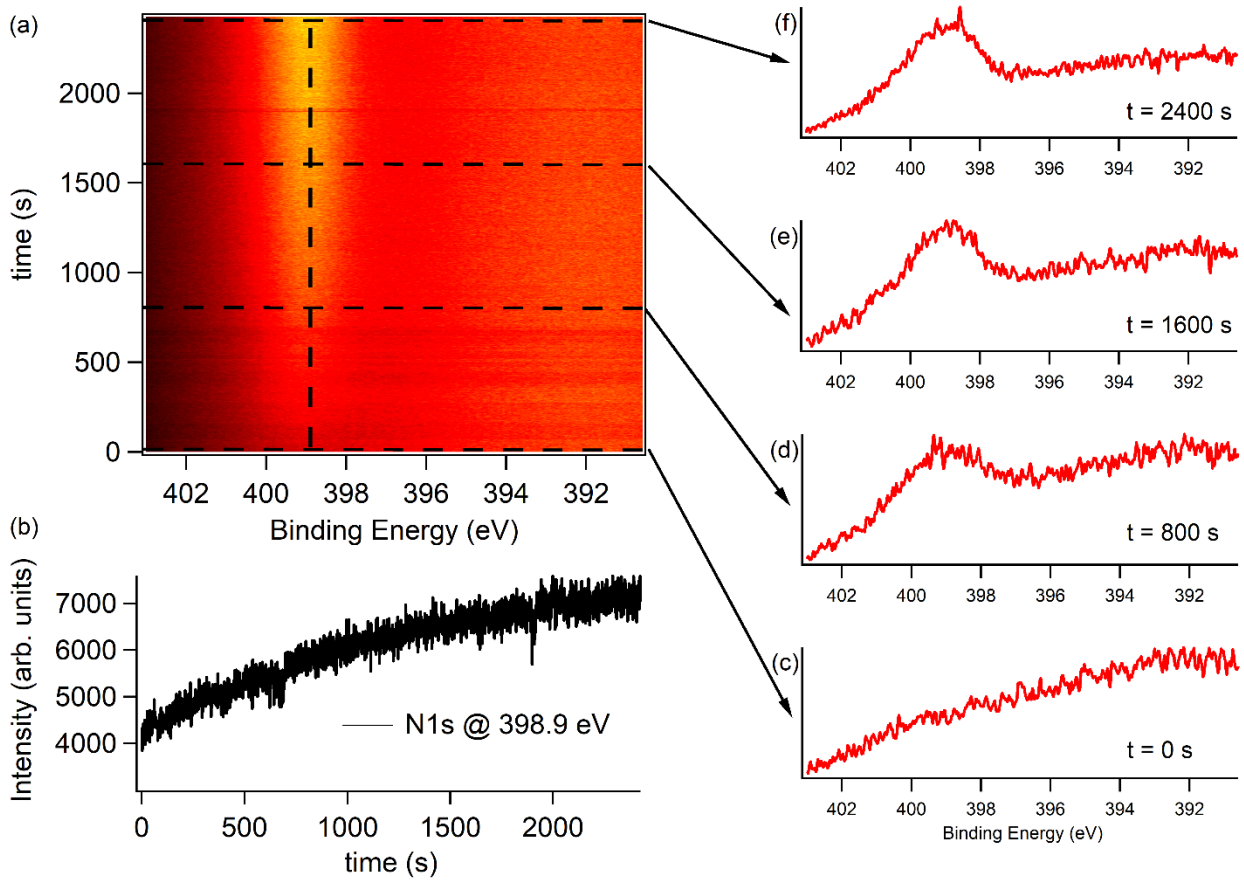

Figure 7: (a) Two dimensional fast XPS spectra of the N 1s level acquired at RT during NH_3 dosing at ~10^{-7} mbar of the C/ZnO hybrid grown at ~800 °C (black: minimum intensity, yellow maximum intensity). Each spectrum has been acquired in ~300 ms, using the analyzer fixed-energy mode, and

a PE=100 eV. (b) Vertical line profile showing XPS signal versus time related to peak energy of 398.9 eV. (c-f) Selected single spectra at different time during gas exposure.

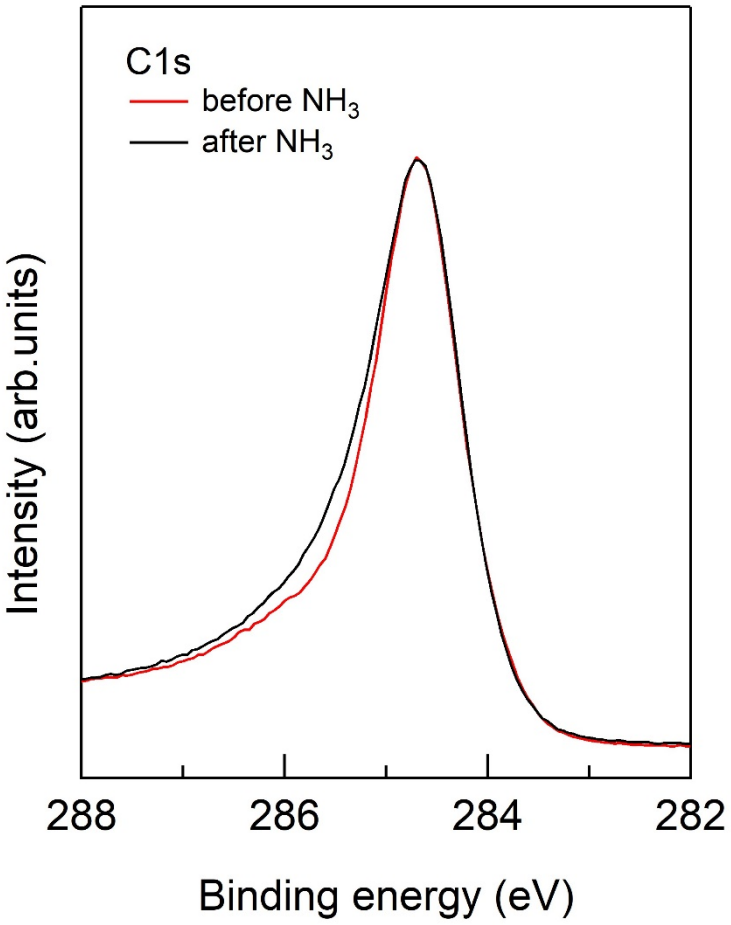

Figure 8: XPS spectra of the C 1s level of the C/ZnO hybrid, before (red) and during (black) ~10^{-7} mbar ammonia exposure.

It was also noted that, when the C/ZnO hybrid was exposed to ammonia, the intensity of the chemisorbed NH_x species in N 1s spectrum gradually increased, unlike the case of bare NRs, where a fast conversion of physisorbed ammonia into cracked species, such as -NH_x, was observed. The sample did not reach saturation even after ~2400 seconds of ammonia gas exposure. This may be attributed to the difference in morphology of the two samples. Figure 1 shows that the hybrid is highly porous and requires a longer time to reach saturation, unlike the solid ZnO NRs. In addition, XPS is a surface sensitive technique: it only measures the N 1s uptake on the surface and not in the bulk. The

apparent slower response does not imply a slower and/or weaker response of these materials in their bulk electronic properties, as will be shown by resistivity measurements in the next section.

3.3 Adsorption isotherms

During ammonia gas exposure, the sample electrical resistance variation was recorded. Figure 9 shows the resistance versus time during NH_3 gas exposure (a, b); ammonia partial pressure (grey dashed line) and dose (black solid line) versus time (c, d); resistance relative response versus dose (e, f) are shown, for bare ZnO NRs and C/ZnO sample, respectively. It should be noted that the response $\Delta R/R_0$ of the C/ZnO hybrid sample is in general higher than for the bare ZnO NRs. In particular, at 400 L the response $\Delta R/R_0$ of the C/ZnO hybrid is nearly one order of magnitude larger than for the bare ZnO NRs.

To analyze these results, we plotted the sample resistance variation versus the dose (L) of the gas calculated by the integral of the partial pressure of gas versus time. If we assume that the response $\Delta R/R_0$ is proportional to the amount of molecules adsorbed on the surface, and since the partial pressure is proportional to the dose of the gas injected in the chamber, we can relate the curves displayed in Figure 9 to the NH_3 adsorption isotherms on the two different surfaces. Under this assumption, we observe that the measured isotherms (Figure 9e-f) are quite different in the two cases. For the ZnO NR (Figure 9e) the isotherm steadily increases and reaches a saturation at 400 L, while for the C/ZnO hybrid (Figure 9f) the isotherm displays two steps in the 0-400 L range. These differences are usually ascribed to the different surface morphologies and are used for the classification of gas-solid adsorption isotherms. Isotherms are classified according to the IUPAC scheme into six different plots, depending on the mechanisms underlying the adsorption process and the morphology of the solid [33]. In the present case the $\Delta R/R_0$ vs dose curves resembles those classified as type I (ZnO NR, Figure 9e) and type VI (C/ZnO hybrid, Figure 9f). Though a detailed study of the adsorption isotherms goes beyond the scope of the present study, we wish to observe that the curve of Figure 9f displays features quite similar to those observed for NH_3 adsorption on

mesoporous carbon [16], indicating that the response to gas is likely dominated by the nanostructured carbon layer in this sample.

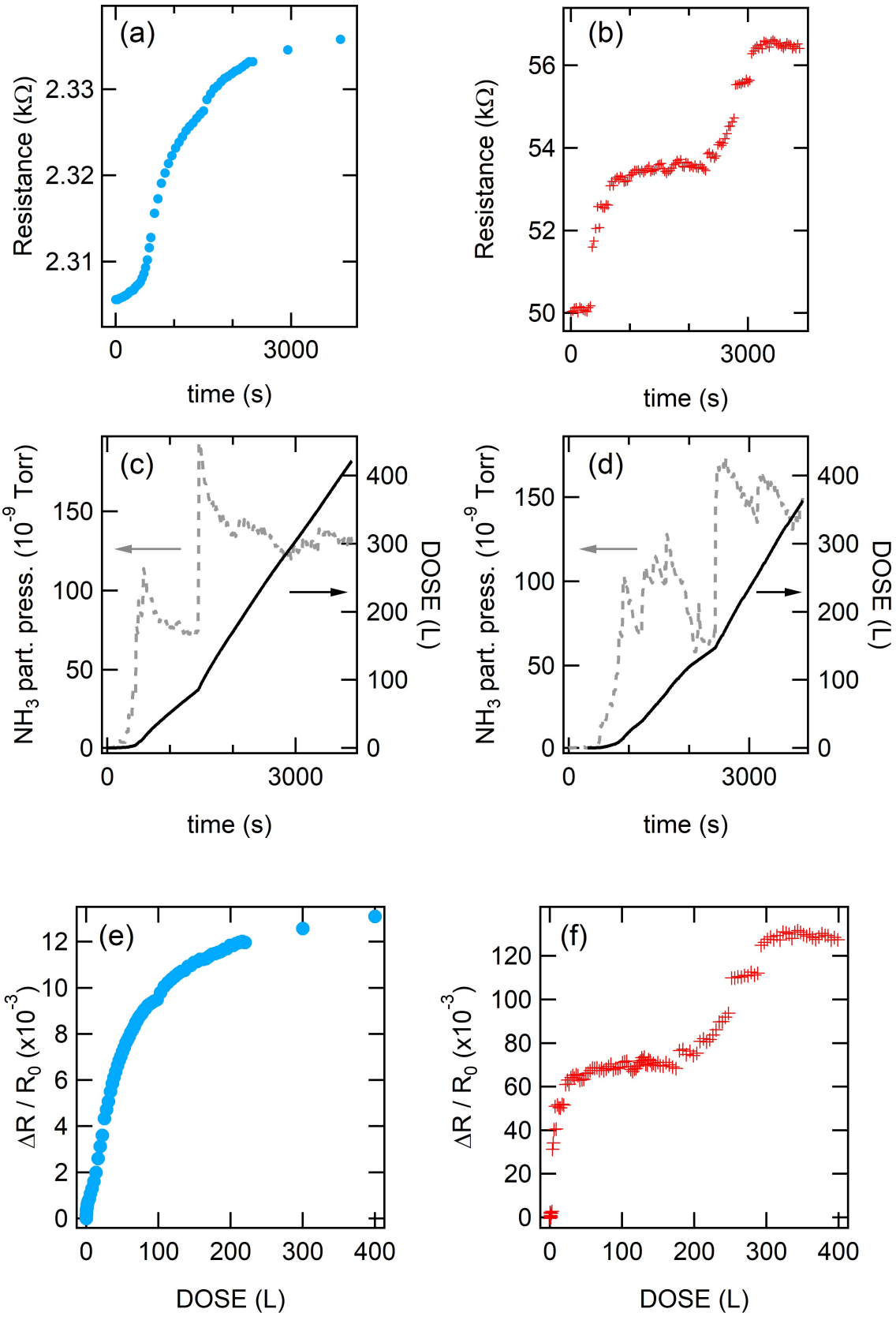
(a)
Resistance (kΩ)
2.33
2.32
2.31
0
3000
time (s)
(b)
Resistance (kΩ)
56
54
52
50
0
3000
time (s)
(c)
NH3 part. press. (10-9 Torr)
150
100
50
0
DOSE (L)
400
300
200
100
0
0
3000
time (s)
(d)
NH3 part. press. (10-9 Torr)
150
100
50
0
DOSE (L)
400
300
200
100
0
0
3000
time (s)
(e)
ΔR / R0 (x10-3)
12
10
8
6
4
2
0
0
100
200
300
400
DOSE (L)
(f)
ΔR / R0 (x10-3)
120
100
80
60
40
20
0
0
100
200
300
400
DOSE (L)

Figure 9: Resistance versus time during NH_3 gas exposure (a, b); ammonia partial pressure (grey dashed line) and dose (black solid line) versus time (c, d); resistance relative response versus dose (e, f) for bare ZnO NRs and C/ZnO sample, respectively.

As reported in the literature, type I physisorption isotherms are given by microporous solids [17]. A microporous material, as classified by the IUPAC, is a material containing pores with diameter less than 2 nm. Consistent with the SEM observation of the ZnO NRs reported in Figure 1a, and the adsorption isotherm in Figure 9e, physisorption from a microporous solid adsorbent is occurring. NH_3 molecules physysorb on the ZnO NRs, i.e. they cover the nanorods surface, without being chemisorbed, until saturation is reached. Type VI isotherms show that adsorption isotherms can have one or more steps [33] and represent multilayer adsorption [17]. From Figure 9f we observe the same curve shape of an isotherm of type VI, which leads us to consider that a multilayer adsorption process is occurring. Consistent with the fast XPS data reported in Figure 7, which shows the predominance of peaks related to NH_3 decomposition products (or chemisorption), the isotherm curve in Figure 9f can be interpreted as a type VI isotherm with a multilayer NH_3 adsorption. Having in mind the morphology (Figure 1b) of the hybrid C/ZnO nanostructures, the fast XPS and adsorption isotherms data, the process occurred most likely as following: after the first layer adsorbed on top of the surface, NH_3 molecules decompose, making free space, i.e. new free adsorption sites, for other NH_3 gas to be adsorbed again. These considerations could also justify the higher sensitivity in terms of electrical resistance variation, and it opens up the possibility of using such C/ZnO nanostructures for gas sensing and ammonia storage.

4. Conclusions

Fast XPS experiments with synchrotron radiation have been carried out in order to track the interaction of ammonia with hybrid materials based on ZnO nanorods and nanostructured carbon. Direct evidence of NH_3 adsorption on nanostructured hybrid interfaces is provided, combined with

transport measurements during the exposure. This operando methodology allowed us to track the adsorption isotherms and relate the different behavior to the sample morphology at the nanoscale. The behaviour of the ZnO nanorods is similar to that observed for physisorption on microporous solids and of the C/ZnO hybrid to chemisorption on mesoporous carbon. While on bare ZnO nanorods, physisorption of ammonia is detected, along with photon beam assisted cracking, on the nanostructured carbon the formation of amine groups is detected, without displaying any effects induced by photon beam exposure. The response $\Delta R/R_0$ of the C/ZnO sample to NH_3 exposure is found to be higher than for the bare ZnO nanorods, suggesting that the C/ZnO hybrid can be regarded as a promising material for gas sensing or for ammonia storage and transportation.

Acknowledgements

This work was supported by the National Research Foundation, South Africa and by the ICTP/IAEA STEP program.

References

[1] A. Goldoni, V. Alijani, L. Sangaletti, L. D'Arsiè, Advanced promising routes of carbon/metal oxides hybrids in sensors: A review, Electrochimica Acta 266 (2018) 139-150.

[2] B.-Y. Wei, M.-C. Hsu, P.-G. Su, H.-M. Lin, R.-J. Wu, H.-J. Lai, A novel SnO2 gas sensor doped with carbon nanotubes operating at room temperature, Sensors and Actuators B: Chemical 101 (2004) 81-89.

[3] N.D. Hoa, N. Van Quy, D. Kim, Nanowire structured SnOx–SWNT composites: high performance sensor for NOx detection, Sensors and actuators B: Chemical 142 (2009) 253-259.

[4] A. Sharma, M. Tomar, V. Gupta, Room temperature trace level detection of NO 2 gas using SnO 2 modified carbon nanotubes based sensor, Journal of Materials Chemistry 22 (2012) 23608-23616.

[5] S. Mubeen, M. Lai, T. Zhang, J.-H. Lim, A. Mulchandani, M.A. Deshusses, N.V. Myung, Hybrid tin oxide-SWNT nanostructures based gas sensor, Electrochimica Acta 92 (2013) 484-490.

[6] J. Yoon, K.W. Min, J. Kim, G.T. Kim, J.S. Ha, p–n hetero-junction diode arrays of p-type single walled carbon nanotubes and aligned n-type SnO2 nanowires, Nanotechnology 23 (2012) 265301.

[7] H.C. Su, M. Zhang, W. Bosze, N.V. Myung, Tin dioxide functionalized single-walled carbon nanotube (SnO2/SWNT)-based ammonia gas sensors and their sensing mechanism, Journal of The Electrochemical Society 161 (2014) B283-B290.

[8] F. Rigoni, G. Drera, S. Pagliara, E. Perghem, C. Pintossi, A. Goldoni, L. Sangaletti, Gas sensing at the nanoscale: engineering SWCNT-ITO nano-heterojunctions for the selective detection of NH3 and NO2 target molecules, Nanotechnology 28 (2016) 035502.

[9] J. Khanderi, R.C. Hoffmann, A. Gurlo, J.J. Schneider, Synthesis and sensoric response of ZnO decorated carbon nanotubes, Journal of Materials Chemistry 19 (2009) 5039-5046.

[10] D. Bai, Z. Zhang, K. Yu, Synthesis, field emission and glucose-sensing characteristics of nanostructural ZnO on free-standing carbon nanotubes films, Applied Surface Science 256 (2010) 2643-2648.

[11] R. Vyas, S. Sharma, P. Gupta, A.K. Prasad, A. Tyagi, K. Sachdev, S. Sharma, CNT-ZnO nanocomposite thin films: O2 and NO2 sensing, Advanced Materials Research, Trans Tech Publ, 2012, pp. 235-239.

[12] W.C. Huang, H.J. Tsai, T.C. Lin, W.C. Weng, Y.C. Chang, J.L. Chiu, J.-J. Lin, C.F. Lin, Y.-S. Lin, H. Chen, Incorporation of carbon nanotube and graphene in ZnO nanorods-based hydrogen gas sensor, Ceramics International 44 (2018) 12308-12314.

[13] R.J. Oweis, B. Albiss, M. Al-Widyan, M.-A. Al-Akhras, Hybrid zinc oxide nanorods/carbon nanotubes composite for nitrogen dioxide gas sensing, Journal of electronic materials 43 (2014) 3222-3228.

[14] Z. Li, B. Gu, A.G. Manohari, C. Xu, Hybrid Structures of Carbon Fiber/ZnO Nanorods and Their Application on Enzyme-Free Sensors for H2O2, Journal of Nanoelectronics and Optoelectronics 13 (2018) 449-453.

[15] C. Petit, K. Kante, T.J. Bandosz, The role of sulfur-containing groups in ammonia retention on activated carbons, Carbon 48 (2010) 654-667.

[16] A. Qajar, M. Peer, M.R. Andalibi, R. Rajagopalan, H.C. Foley, Enhanced ammonia adsorption on functionalized nanoporous carbons, Microporous and Mesoporous Materials 218 (2015) 15-23.

[17] K.S. Sing, Reporting physisorption data for gas/solid systems with special reference to the determination of surface area and porosity (Recommendations 1984), Pure and applied chemistry 57 (1985) 603-619.

[18] J. Wang, X. Sun, Y. Yang, H. Huang, Y. Lee, O. Tan, L. Vayssieres, Hydrothermally grown oriented ZnO nanorod arrays for gas sensing applications, Nanotechnology 17 (2006) 4995.

[19] P. Mbuyisa, O. Ndwandwe, C. Cepek, Controlled growth of zinc oxide nanorods synthesised by the hydrothermal method, Thin Solid Films 578 (2015) 7-10.

[20] P. Mbuyisa, S.P. Bhardwaj, F. Rigoni, E. Carlino, S. Pagliara, L. Sangaletti, A. Goldoni, M. Ndwandwe, C. Cepek, Controlled synthesis of carbon nanostructures using aligned ZnO nanorods as templates, Carbon 50 (2012) 5472-5480.

[21] G. Drera, G. Salvinelli, J. Åhlund, P. Karlsson, B. Wannberg, E. Magnano, S. Nappini, L. Sangaletti, Transmission function calibration of an angular resolved analyzer for X-ray photoemission spectroscopy: Theory vs experiment, Journal of Electron Spectroscopy and Related Phenomena 195 (2014) 109-116.

[22] A. Wei, X.W. Sun, C. Xu, Z.L. Dong, Y. Yang, S. Tan, W. Huang, Growth mechanism of tubular ZnO formed in aqueous solution, Nanotechnology 17 (2006) 1740.

[23] N.S. Ramgir, D.J. Late, A.B. Bhise, M.A. More, I.S. Mulla, D.S. Joag, K. Vijayamohanan, ZnO multipods, submicron wires, and spherical structures and their unique field emission behavior, The Journal of Physical Chemistry B 110 (2006) 18236-18242.

[24] E. De la Rosa, S. Sepulveda-Guzman, B. Reeja-Jayan, A. Torres, P. Salas, N. Elizondo, M.J. Yacaman, Controlling the growth and luminescence properties of well-faceted ZnO nanorods, The Journal of Physical Chemistry C 111 (2007) 8489-8495.

[25] Z. Li, Y. Xiong, Y. Xie, Selected-control synthesis of ZnO nanowires and nanorods via a PEG-assisted route, Inorganic chemistry 42 (2003) 8105-8109.

[26] P. Davies, N. Newton, The chemisorption and decomposition of pyridine and ammonia at clean and oxidised Al (1 1 1) surfaces, Surface science 546 (2003) 149-158.

[27] C. Bater, M. Sanders, J. Craig Jr, Electron-stimulated dissociation of ammonia adsorbed on Ge (100), Surface science 451 (2000) 226-231.

[28] K. Ozawa, T. Hasegawa, K. Edamoto, K. Takahashi, M. Kamada, Adsorption state and molecular orientation of ammonia on ZnO (1010) studied by photoelectron spectroscopy and near-edge X-ray absorption fine structure spectroscopy, The Journal of Physical Chemistry B 106 (2002) 9380-9386.

[29] J. Lin, P.M. Jones, M.D. Lowery, R.R. Gay, S.L. Cohen, E.I. Solomon, Coordination chemistry of ammonia on zinc oxide (0001) and cuprous chloride (111) surfaces:. sigma.-bonding interactions with d10 metal ion sites, Inorganic Chemistry 31 (1992) 686-695.

[30] C. Egawa, S. Naito, K. Tamaru, Adsorption and decomposition of ammonia on W (100); XPS and UPS studies, Surface science 131 (1983) 49-60.

[31] A.J. Bishop, A.F. Carley, P. Roussel, P. Nevitt, The adsorption of ammonia on polycrystalline thorium, Radiochimica Acta 97 (2009) 243-246.

[32] J.-M. Tulliani, A. Cavalieri, S. Musso, E. Sardella, F. Geobaldo, Room temperature ammonia sensors based on zinc oxide and functionalized graphite and multi-walled carbon nanotubes, Sensors and Actuators B: Chemical 152 (2011) 144-154.

[33] M. Donohue, G. Aranovich, Classification of Gibbs adsorption isotherms, Advances in colloid and interface science 76 (1998) 137-152.